Materials Research. 2017; 20(Suppl. 2): 331-341
DOI: http://dx.doi.org/10.1590/1980-5373-MR-2016-1012

Analysis of Compositional Modification of Commercial Aluminum Bronzes to Obtain Functional Shape Memory Properties

Aylanna Priscila Marques de Araujo[a]*, Jackson de Brito Simões[b], Carlos José de Araújo[c]

[a]Departmento of Materials Engineering, Universidade Federal de Campina Grande, Av. Aprígio Veloso, 882, CEP 58429-140, Campina Grande, PB, Brazil.
[b]Universidade Federal Rural do Semi-Árido, RN 233, km 01, Sítio Esperança II Zona rural, CEP 59780-000, Caraúbas, RN, Brazil.
[c]Department of Mechanical Engineering, Universidade Federal de Campina Grande, Av. Aprígio Veloso, 882, CEP 58429-140, Campina Grande, PB, Brazil.

Received: December 12, 2016; Revised: July 17, 2017; Accepted: July 21, 2017

In copper-based shape memory alloys (SMAs), some exceptional phenomena, such as the shape memory effect (SME) or superelasticity (SE), are observable. However, commercial aluminum bronzes, Cu_3Al-based alloys, do not present these functional properties (SME and/or SE) in their original state. Thus, since one of the main copper-based SMA systems is the Cu-Al-Ni alloy, this paper aims to analyze the modification of these commercial aluminum bronzes to SMA by the addition small amounts of Cu, Al and/or Ni. These modified bronzes were reprocessed by induction melting and injected by centrifugation into a ceramic coating mold. The modifications were made to determine the nominal composition for a Cu-13,0Al-4,0Ni (%wt) SMA. The effectiveness of the modifications was verified by differential scanning calorimetry (DSC) thermal analysis. All modified Cu-Al-Ni bronzes presented DSC peaks of the thermoelastic martensitic phase transformation, showing that SMA behavior was achieved, while the non-modified bronzes revealed no transformation. These results were supported by Vickers hardness (HV), X-ray diffraction (XRD), semi quantitative composition by EDS analysis and optical microscopy.

Keywords: *Bronze, Shape memory alloys, Cu-Al-Ni alloys, Thermoelastic martensitic phase transformation.*

1. Introduction

Shape memory alloys (SMAs) are special metallic materials that present the functional phenomena of the shape memory effect (SME) and superelasticity (SE); thus, they are classified as active or smart metals. Both phenomena occur due to the thermoelastic martensitic phase transformation. The SMA undergoes a reversible martensitic transformation, allowing deformation through a twinning mechanism when temperatures are below the final martensite transformation limit (M_f)[1]. For the SME, this deformation is reversed when the detwinned structure (martensite) transforms to a parent phase above the initial austenite transformation temperature (A_s) through heating. Cu-Al binary alloys show a martensitic transformation with high transformation temperatures. However, these temperatures can be adjusted by adding a third element to the alloy. The addition of up to 4 %wt. nickel reduces the transformation temperatures of Cu-Al alloys[1,2]. The nickel acts to retard the diffusion of aluminum in annealed Cu-Al alloys, eliminating the stable γ_2 phase that does not undergo the martensitic transformation. It is also known that the transformation temperatures of these alloys are sensitive to their chemical composition[1-4]. For the Cu-XAl-4Ni alloys (% wt), it has been observed that the transformation temperatures abruptly decrease with a slight increase in Al content (X)[1,5]; depending on the Al content, different martensites can be formed, denoted as γ_1' or β_1' [3,6].

Copper-based SMA have steadily attracted the attention of researchers during recent decades due to their low cost and ease of manufacturing when compared with TiNi - based alloys[1,4]. From this knowledge and noting that commercial aluminum bronzes are basically Cu_3Al - based alloys that have a number of other trace elements (Ni, Fe, Mn and others) in their composition[7], the aim of this study was to investigate whether these bronzes can present a phase transformation in the as supplied state after quenching. If not, thus study sought to assess the possibility of minimally altering its chemical composition for the thermoelastic martensitic transformation to occur, which is the origin of the functional SME phenomena.

It is important to note that an attempt to modify commercial aluminum bronzes to obtain properties of the thermoelastic phase transformation and the shape memory effect has not been found in the international literature.

*e-mail: aylannapriscila@hotmail.com

2. Materials and Methods

2.1 Materials

The materials used in this study were three commercial aluminum bronze alloys supplied by Metals Luna Company (São Paulo, Brazil): BRONZE AL NI CA 9581 C95800; BRONZE SAE 630 C63000 and BRONZE SAE 68D C95500. Due to the lack of identification, these bronzes were named A, B and C, respectively.

2.2 Methods

Initially, the supplied aluminum bronzes were subjected to a heat treatment at 850°C for 30 minutes, followed by quenching in water at approximately 30°C. After this treatment, the aluminum bronzes were cut into samples of a mass between 20 and 100 mg to be investigated in the DSC thermal analysis using a Q20 model calorimeter (TA Instruments). As these first DSC analyzes did not reveal the occurrence of phase transformation peaks, the samples of each kind of bronze were subjected to a chemical analysis using energy dispersive spectroscopy (EDS) in a scanning electron microscope (SEM) VEGA3 model (Tescan) equipped with an EDS detector from Oxford Instruments (Oxford Instruments, X-act model). The magnification used was set at 2000x, and a total of 5 EDS measurements were taken at 5 random points for each sample. The compositions of the aluminum bronzes (as supplied) by weight (%wt.) from the EDS are summarized in Table 1.

According to this preliminary composition analysis for each bronze alloy, the new set of modified bronzes for an SMA nominal composition of Cu-13,0Al-4,0Ni (%wt.) was established based on the literature data[1,5]. For this, considering that the total mass to produce the new Cu-Al-Ni SMA specimens was 40 g, a mass correction of the elements for each of the as received bronze alloys (A, B and C) was performed, as shown in Table 2. The complementary elements for the production of modified bronzes (Cu-Al-Ni SMA) were cut according to the calculated masses shown in Table 2.

The modified bronzes were produced using the Powercast 1700 machine, from EDG equipment and controls (São Paulo, Brazil), which uses the induction melting technique with injection by centrifugation into a ceramic mold. At the end of the melting and injection process, the ceramic mold is removed from the machine and rapidly cooled in water. Once cleaned and prepared, samples were subjected to a heat treatment at 850°C for 30 minutes (betatization) followed by quenching in room temperature water. A specific nomenclature was given to identify the new modified aluminum bronze alloys, which can be seen in Table 3.

All modified aluminum bronzes were first characterized by DSC thermal analysis using the same equipment aforementioned (calorimeter Q20 model from TA Instruments). The sample masses for these analyses were between 20 and 100 mg, and the temperature range was from 0°C to 300°C with a heating/cooling rate of 20°C/min under a nitrogen atmosphere. The starting and final transformation temperatures, both during cooling and heating, were obtained by the tangent intersection method of the DSC peaks[1].

Vickers hardness (HV) measurements were carried out using a FM-700 equipment from Future-Tech. All indentations were performed at room temperature with a load of 300 gf and an application time of 15 s. One sample of each bronze

Table 1. Chemical composition (%wt.) of the as received commercial aluminum bronzes obtained by EDS.

Bronze ↓	Cu	Al	Ni	Fe	Mn	Si	Zn
A	69.45	7.55	3.71	14.18	1.28	12.83	1.48
B	72.95	9.64	6.16	7.15	0.97	--	12.83
C	78.39	11.43	5.42	3.32	0.74	0.48	12.83

Table 2. Correction for the compositional aluminum bronzes A, B and C with a total mass of 40 g and the Cu-13.0Al-4.0Ni SMA.

Bronze ↓	As received bronze (g)	Cu added (g)	Al added (g)	Ni added (g)
A	37.5	--	2.381	0.212
B	26.0	11.341	2.699	--
C	30.0	8.795	1.856	--

Table 3. Nomenclature used for bronze alloy modified during execution of the work.

Conditions of the Bronze Alloy	A	B	C
As received	A	B	C
As received and quenched	AT	BT	CT
As modified	AMB	BMB	CMB
As modified and quenched	AMT	BMT	CMT

(both the as supplied and for modified) was used, and each sample was subjected to 10 indentations in random points.

For the identification of the phases present in the aluminum bronzes, the XRD technique was employed using a diffractometer XRD-6000 Model from Shimadzu. The Cu-K_α radiation was used with a 2Θ interval from 20 to 90° and scanning steps of 0.02° with 3 s of accumulation.

The microstructures were observed by optical microscopy (OM). The etching solution used for these observations was 10 g $FeCl_3$ + 25 mL HCl + 100 mL H_2O. The images were captured using an Olympus microscope, model BX51M.

3. Results and Discussion

3.1 Verification of phase transformation by Differential Scanning Calorimetry (DSC)

DSC analyses were performed for the aluminum bronze alloys under the following conditions: supplied after quenching (AT, BT and CT), modified with no heat treatment (AMB, BMB and CMB) and modified after quenching (AMT, BMT and CMT).

It can be observed from the DSC results shown in Figure 1 that all supplied bronzes showed no phase transformation, even after the heat treatment (quenching). On the other hand, all modified alloys in both conditions (no quenching and after quenching) provided phase transformation peaks. The occurrence of the thermoelastic martensitic phase transformation in all modified bronzes reveal a strong potential for the shape memory effect to be achieved.

Figure 1 also shows that the temperatures of the forward (cooling, M_s and M_f) and reverse (heating, A_s and A_f) transformations have been reduced for all modified bronze alloys after quenching, which is now denoted Cu-Al-Ni SMA. The forward (during cooling) and reverse (during heating) phase transformation temperatures were measured with the method of tangents in the transformation peaks[1]. Table 4 summarizes these phase transformation temperatures of the new Cu-Al-Ni SMA with no heat treatment and after quenching. It is verified that the transformation temperatures decrease with the increase of the aluminum content in the modified bronzes (Cu-Al-Ni SMA), according to the literature[1,5]. By checking Tables 4 and 5, it is noted that the M_s temperature is reduced from 183.8°C in the CMT alloy (9.7 %wt. Al) to only 41.4°C in the AMT alloy (17.0 %wt. Al). According to Chang[5], thermal transformation of the Cu-13,0Al-4,0Ni (%wt.) SMA occurs between 150°C and 210°C, with a M_s temperature on the order of 181°C.

Ten thermal cycles were performed to verify the stability of the phase transformations observed in the new Cu-Al-Ni SMA manufactured in this study. Figure 2 shows the DSC curves for alloys A, B and C (modified and before and after quenching) during the thermal cycling. For the three alloys, well-defined peaks are again observed, confirming the forward (cooling) and reverse (heating) martensitic transformation. The transformation temperatures shifted at each cycle to higher temperatures for alloys A and B. It is well known that thermal cycling up to 200°C may promote not only modifications in the alloy structure and composition but also changes in its physical and mechanical properties[1,6]. Araujo et al.[8] detected an increase in the critical transformation temperatures associated with a change of γ_1' into β_1' martensite after a sufficiently long aging time at 200°C. In our case, and only for alloy C, after an increase during the first seven thermal cycles, the transformation temperatures shifted to lower values. The enthalpies of transformation also decreased, indicating that the phase transformation for this particular alloy tends to disappear with thermal cycling between 0°C and 300°C. This is caused by the fact that the modified alloy C presents the highest transformation temperatures A_s and A_f between 200°C and 250°C. This behavior was also observed for the Cu-Al-Nb SMA, where after the fifth thermal cycle, at temperatures higher than 250°C, the phase transformation tends to disappear completely. The low thermal stability observed in the alloys of the Cu-Al-Nb system is due to intense development of the diffusion processes at relatively high temperatures of the cycled heating[9]. This is probably the case for our modified alloy C (CMT). However, after disappearance after a few cycles to a maximum temperature of 300°C, the phase transformation can be recovered by a new heat treatement (quenching), so that the material (Cu-Al based SMA) can be reused for a few more thermal cycles.

The aforementioned variation in the transformation temperatures for alloys A, B and C in the modified and quenched condition can be best seen in Figure 3. An increase of the peak temperatures was observed for both the forward (M_p) and reverse transformation (A_p), as well as the stability of the thermal hysteresis behavior ($H_t = A_p - M_p$) during the cycling, except for alloy C beginning at the eighth cycle, as previously described.

The behavior of the forward (ΔH_{A-M}) and reverse (ΔH_{M-A}) transformation enthalpies (in J/g) can be seen in Figure 4. For the modified alloys AMT and BMT, a slight difference between the forward and reverse transformations was observed. Moreover, neither enthalpies are practically affected by the number of cycles. This is an apparent indication that the alloy thermodynamic states are not influenced by either the direction of transformation or the number of thermal cycles, as also reported by Pereira et al.[6]. Then, a better stability of transformation energies was verified for the modified alloys A and B and a gradual reduction for alloy C due to the thermal degradation associated with the diffusion processes

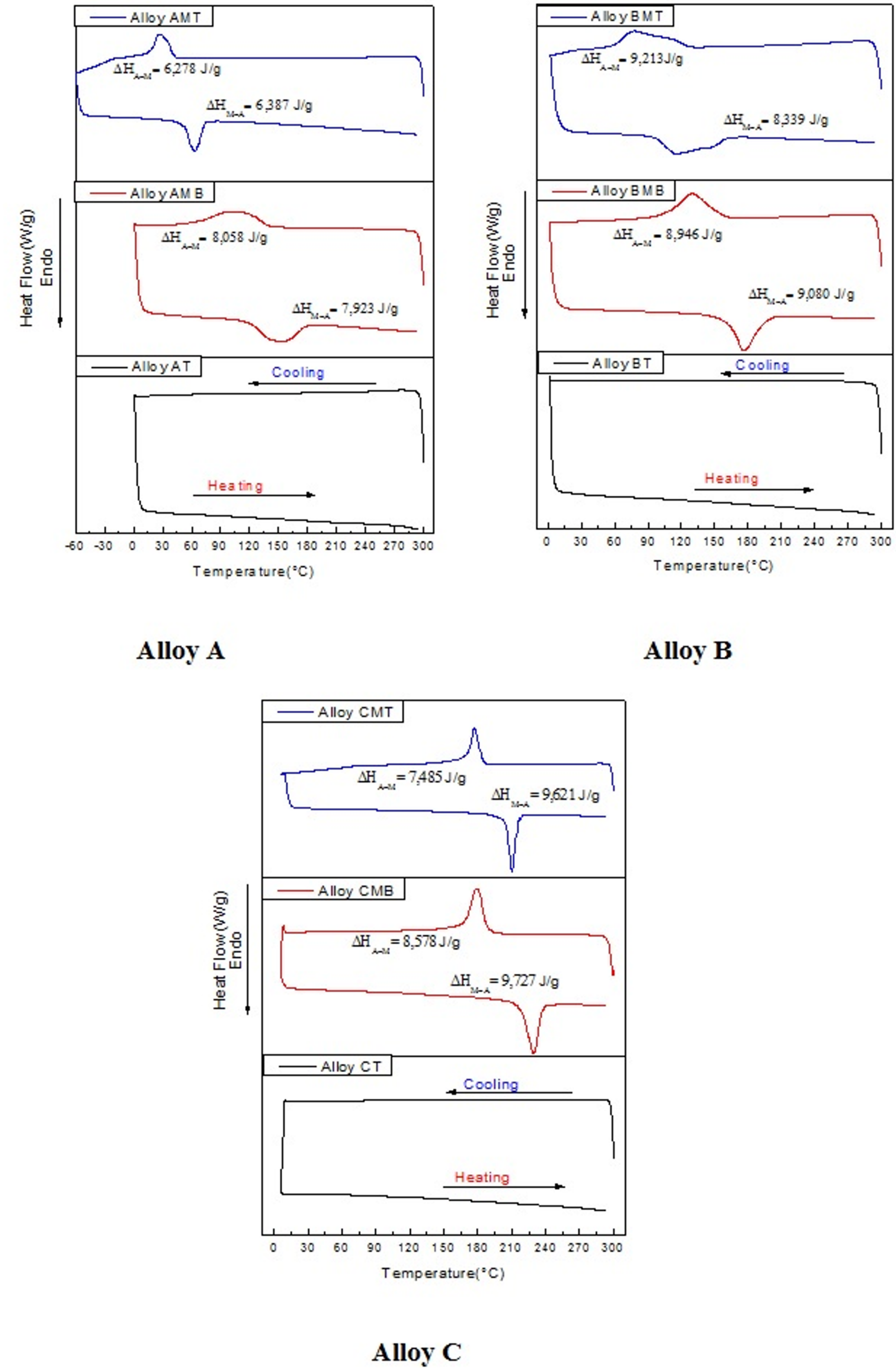

Figure 1. DSC thermal analysis of the as provided and modified bronze alloys (Cu-Al-Ni SMA).

Table 4. Transformation temperatures and thermal hysteresis (ºC) of the modified aluminum bronzes (Cu-Al-Ni SMA).

Cu-Al-Ni ↓	M_S	M_f	A_s	A_f	Hysteresis
AMB	119.1	65.4	119.9	178.5	41.2
AMT	41.4	17.4	53.1	73.1	37.0
BMB	157.6	105.3	163.0	194.1	46.6
BMT	127.1	68.3	111.0	159.2	36.0
CMB	187.9	169.1	219.7	236.8	50.2
CMT	183.8	171.3	205.5	216.0	34.3

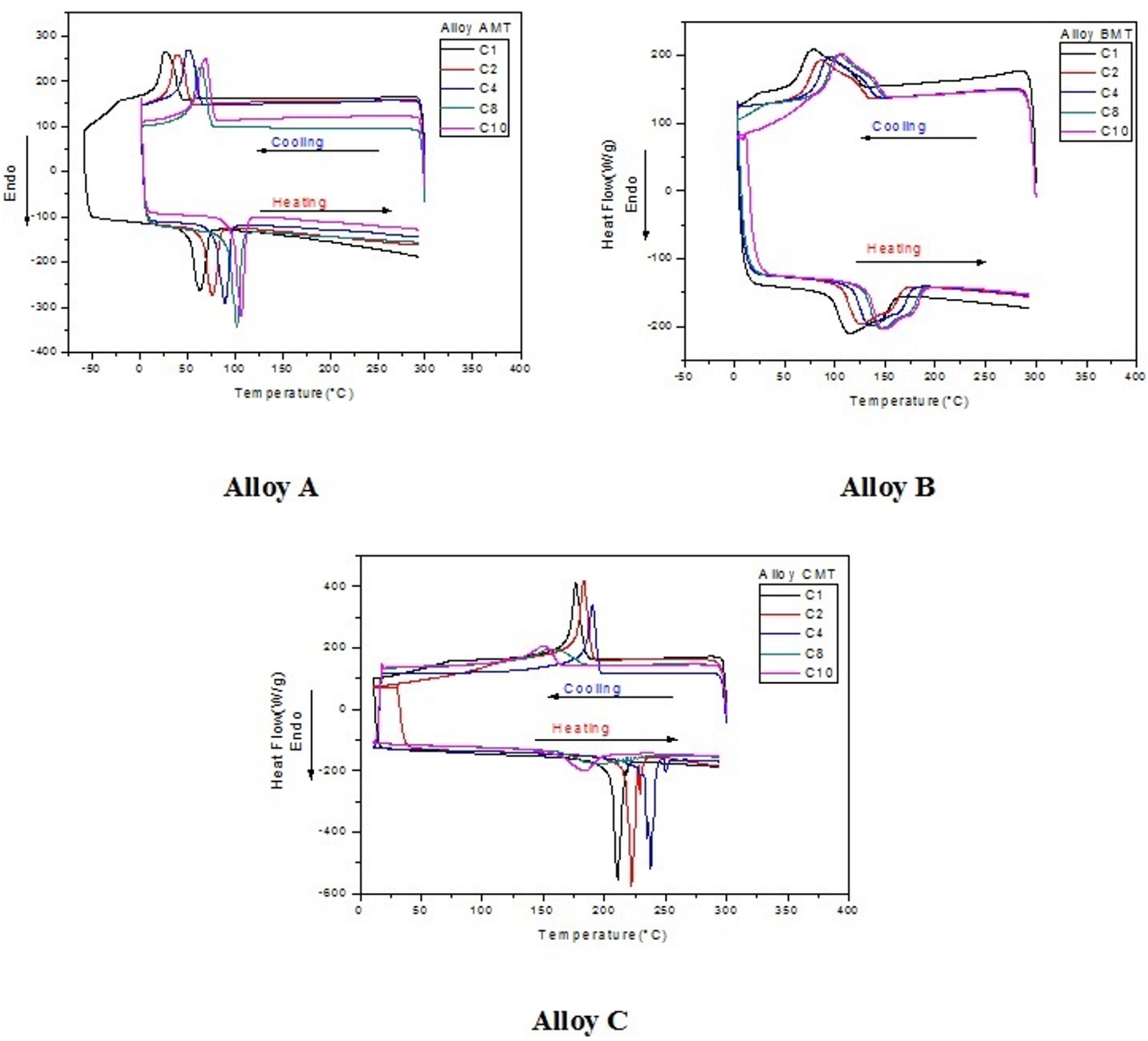

Figure 2. Effects of thermal cycling on the Cu-Al-Ni SMA (modified and quenched).

at relatively high temperatures of cycled heating[9]. For all the modified alloys, it was found that these energies agree with the transformation enthalpies reported in the literature for Cu-Al-Ni SMA with 13.5 to 14.0 %wt. Al in the range of 5 to 10 J/g[1,5,6].

3.2 Mechanical Behavior - Hardness HV

Figure 5 shows the hardness HV values for the aluminum bronze alloys in all studied conditions (as supplied, as supplied then quenched, as modified, and as modified then quenched). It was observed that for all as supplied bronzes, heat treatment (quenching) resulted in an increase in the hardness from 200 HV to 350 HV, in agreement with literature values for nickel-aluminum bronzes[10]. On the other hand, it was found for the modified bronze alloys that the samples before quenching, by the melting process, presented a higher hardness value than the one for the alloys after quenching. This behavior can be explained by the occurrence of a larger amount of

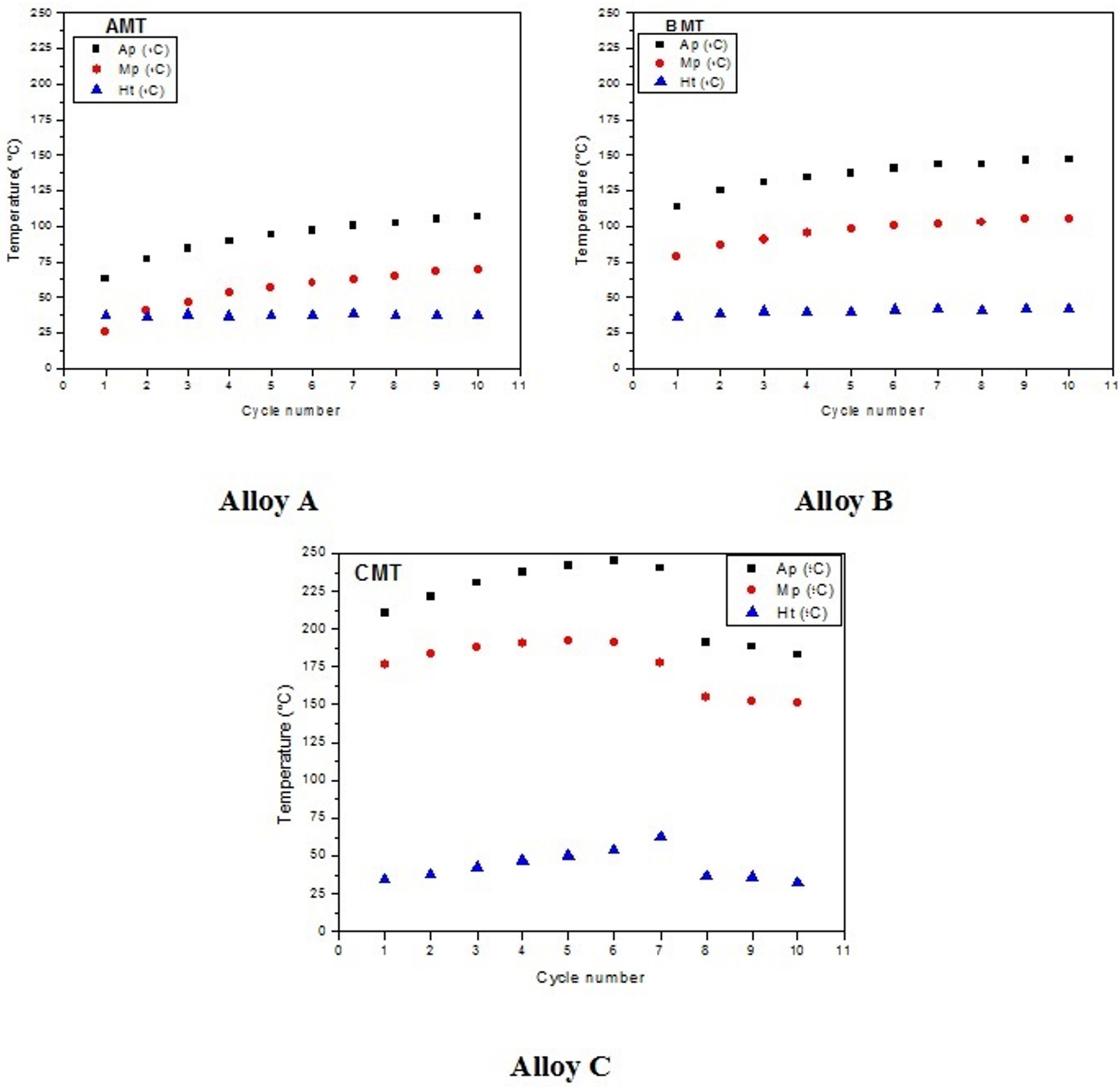

Figure 3. Evolution of the peak temperatures of the transformations and hysteresis during thermal cycling of the Cu-Al-Ni alloys (modified and quenched).

the twinned martensite phase after quenching (γ_1' and β_1' martensites). This level of hardness for the thermoelastic martensitic structure, from approximately 270 HV to 300 HV, is in agreement with values found earlier in the literature for the same Cu-Al-Ni SMA[11].

3.3 X-Ray Diffraction (XRD)

Figure 6 shows XRD patterns obtained at room temperature for the as supplied (Fig. 6a) and modified (Fig. 6b) bronzes, both annealed and quenched. The identification of the XRD peaks was performed based on the literature values for Cu-Al-Ni SMA[3,12]. In Figure 6(a) for the three alloys, the XRD revealed the presence of the α phase (Cu_4Al) with DO_3 ordering and other peaks that were not identifiable. The alloy CT also revealed peaks of the high temperature β phase (Cu_3Al) ordered with a DO_3 structure. On the other hand, for the three Cu-Al-Ni SMA (Fig. 6b), the presence of two types of martensite phases were observed, β_1' (Orthorhombic -18R) and γ_1' (Monoclinic -2H), peaks of the high temperature β phase (Cu_3Al) ordered with a DO_3 structure and the α phase (Cu_4Al) with DO_3 ordering. For the AMT and BMT alloys, the presence of a solid phase rich in aluminum was still detected, γ_2 (Cu_9Al_4), with DO_3 ordering, which is responsible for the brittleness of the

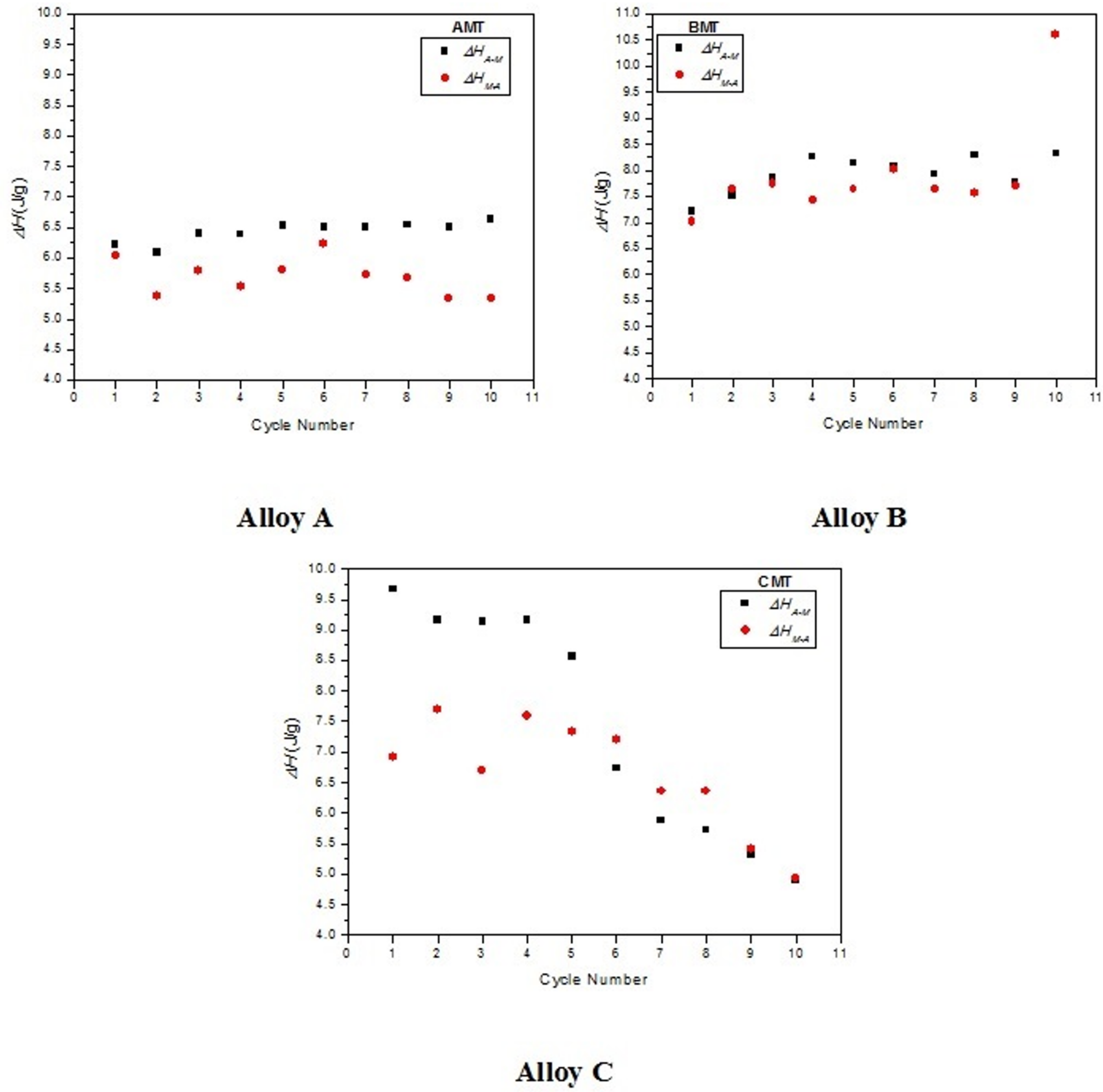

Figure 4. Evolution of the transformation enthalpies during thermal cycling of the of the Cu-Al-Ni alloys (modified and quenched).

Cu-Al-Ni SMA. The deformation of the two-phase domain is impractical due the fragility that the γ_2 phase produces, caused by its inconsistency with the matrix[1]. There is also evidence of another possible precipitate that these alloys may present: the AlNi, which has a B2 ordered type structure[12]. As the martensitic phase type β_1' is less stable than γ_1', the thermal cycling may cause the alloy that contains a higher volume of this phase to lose its SME properties. This occurs due to structural changes and dislocation arrangements at quenching sites that function as seeds for nucleation of the orthorhombic martensite phase β_1'[13].

3.4 Energy Dispersive Spectroscopy (EDS)

The semi-quantitative evaluation of the chemical composition of the modified and quenched aluminum bronze alloys (AMT, BMT and CMT) was obtained by EDS microanalysis carried out in dots and lines. The measurements were statistically treated to obtain the average values, as summarized in Table 5. These values show that the alloys are not identical in composition, as they present different contents of Cu and Al. From these results, it is possible to understand the behavior of the phase transformation temperatures obtained by the DSC for each modified bronze, considering that with the increasing aluminum content, the transformation temperatures decrease[1,8]. This also may explain the occurrence of the γ_2 brittle phase in the alloys with a higher aluminum content (AMT e BMT), as well as its absence in the CMT alloy (Fig. 6b). Comparing the compositions summarized in Table 1 with those in Table 5, it can be seen that after the modification, while the Ni content values maintained

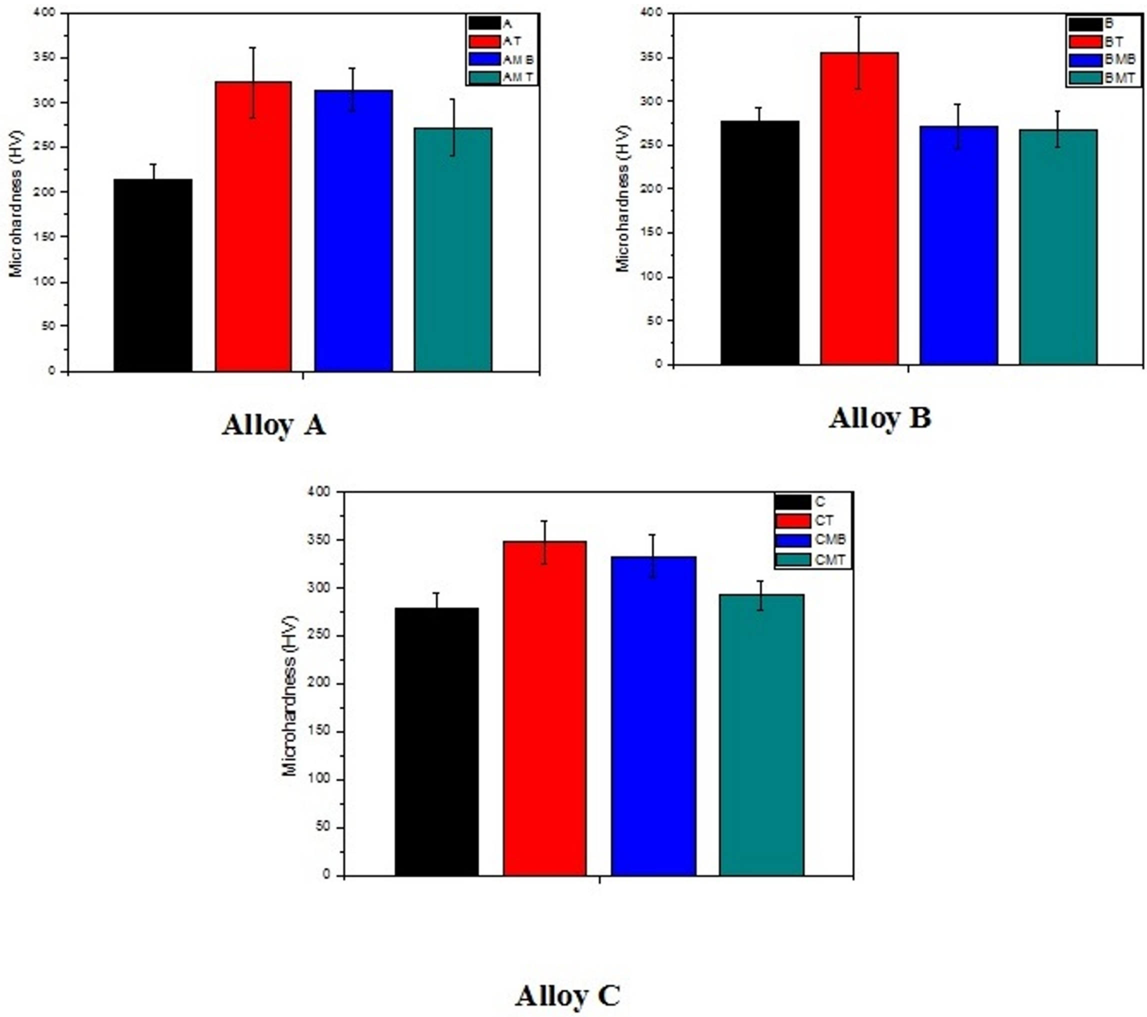

Figure 5. Microhardness values of the studied Cu-Al-Ni alloys.

a correlation to the designed alloy (nominal composition of Cu-13,0Al-4,0Ni SMA), the aluminum content values presented the opposite behavior. Additionally, it should be noted that the reprocessing with the investment casting technique alters the content of the residual elements (Fe, Mn, Si and Zn). The EDS results of the modified and quenched bronzes were statistically compared by a one-way ANOVA. P-values of less than $\alpha=0.05$, as shown in Table 6, indicate significant differences between the content values of the main elements (Al, Cu and Ni).

It is important to note that these aluminum bronzes may have other residual elements, such as Fe and Si[7,10]. In our case, a significant Zn content was also detected (Table 1). In the case of bronze B, the analysis by EDS did not detect the presence of Si, perhaps because it is a semi quantitative technique. After modifying the bronzes by remelting with addition of new amounts of Cu, Al and/or Ni, the compositions undergo a complete rearrangement, including the residual elements Fe, Mn, Si and Zn, as indicated in Table 5. The Zn content is reduced and even disappears in the case of alloy B. This may occur by evaporation of Zn during the modification process which includes a further melting of the bronze. Si appearing in alloy B after modification may be associated with the limitation of the EDS technique on detecting it in the original bronze (alloy B, Table 1).

3.5 Optical Microscopy (OM)

Figure 7 shows the optical micrographs of the studied bronze alloys. The A, B and C alloys present large quantities of the α phase, which is characteristic of aluminum bronzes. This phase is a solid copper-based solution having a CFC structure and formed when the cooling time is sufficient for the occurrence of the phases, according to the phase diagram of the alloy[13]. It can also be observed for the AT alloy that

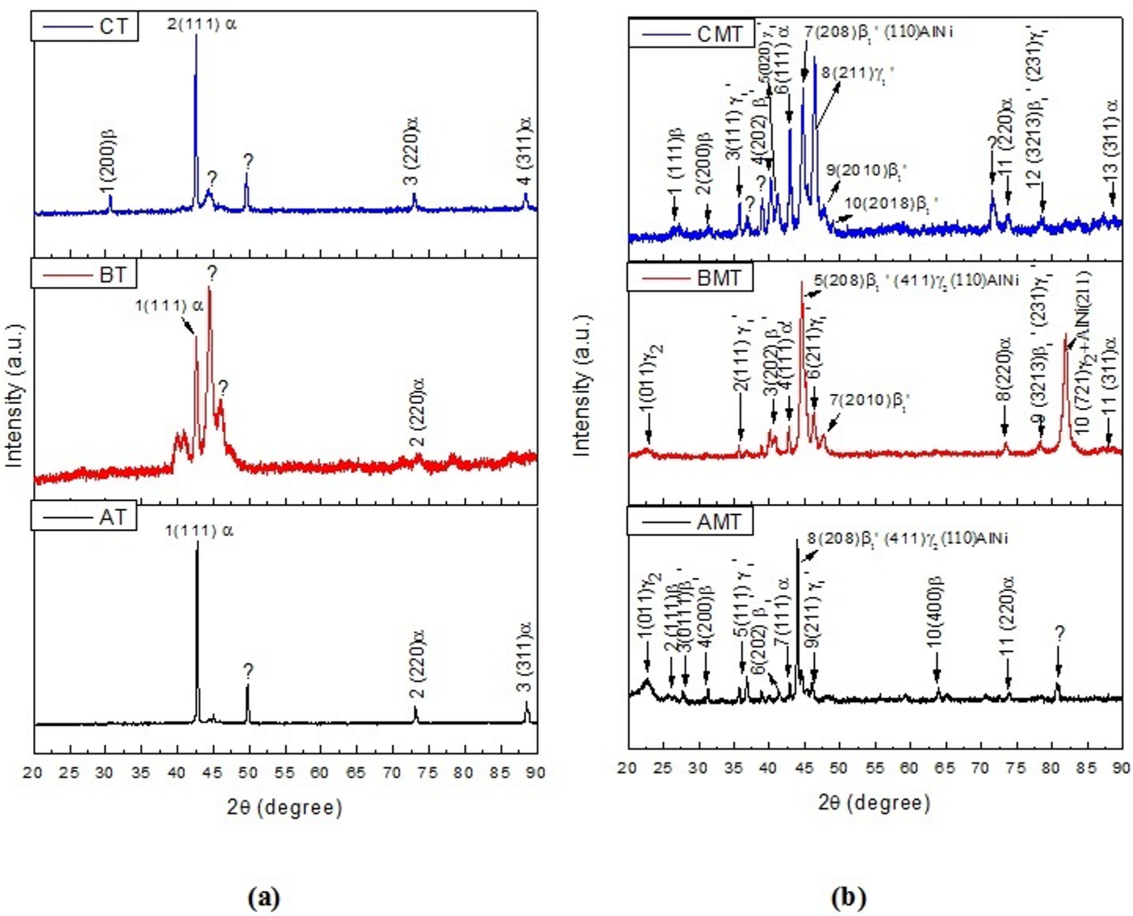

Figure 6. X-ray diffractograms of the studied Cu-Al-Ni alloys. (a) Quenched bronzes (as provided). (b) Modified and quenched Cu-Al-Ni alloys.

Table 5. Chemical composition (%wt.) obtained by EDS for the modified and quenched aluminum bronzes.

Cu-Al-Ni ↓	Cu	Al	Ni	Fe	Mn	Si	Zn
AMT	73.7±0.30	17.0±0.62	4.9±0.21	2.2±0.04	0.7±0.01	0.6±0.27	0.8±0.06
BMT	79.2±0.87	14.2±0.77	3.3±0.01	2.5±0.02	0.5±0.00	0.3±0.09	--
CMT	82.0±0.56	9.7±0.25	4.0±0.01	2.5±0.73	0.6±0.03	0.3±0.07	0.9±0.03

Table 6. Statistical comparison of the EDS results by a one-way ANOVA of the modified and quenched aluminum bronzes (Cu-Al-Ni SMA).

	Cu	Al	Ni
p-Value	0.004	0.001	0.02

the heat treatment of quenching promoted a thin plate shape for the α phase. Whereas for the BT and CT alloys, the microstructures presented coarser grains in the α phase domains. According to Rodrigues[13], the α phase is ductile, and its reduction tends to increase the overall hardness. This fact was also observed through the microhardness analysis in this study. For the other alloys, the presence of the α phase and discrete needles of the martensite β_1' (with structure 18R) was observed on the matrix of the austenite β (with the ordinate structure DO_3). Grain boundaries were observed for the quenched alloys, where possible acicular precipitates still appear scattered. According to Chang[5], these precipitates can correspond to the γ_2 phase, which has a Cu_9Al_4 structure.

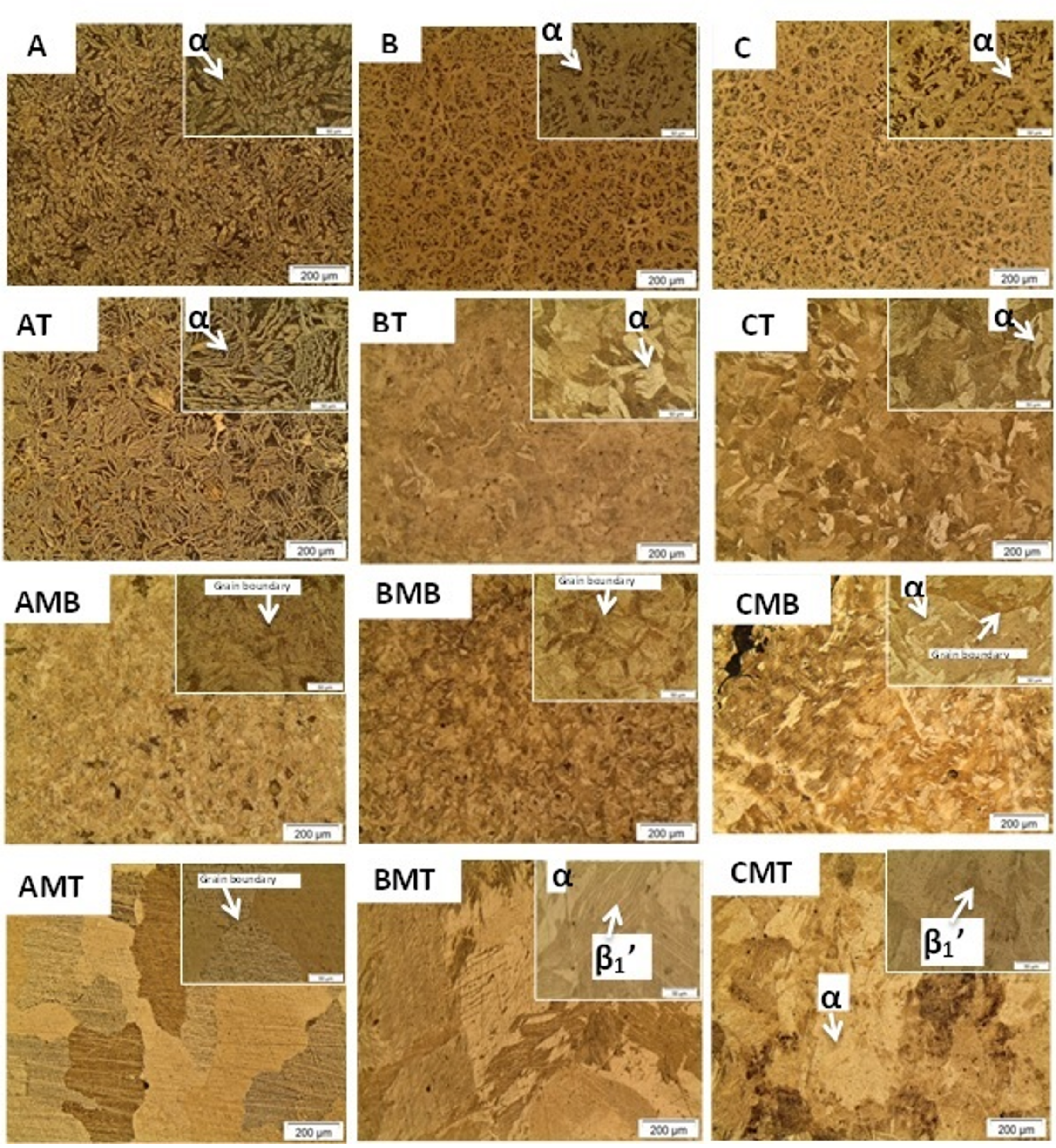

Figure 7. Microstructures of all the studied non-modified and modified bronze alloys (Cu-Al-Ni SMA).

4. Conclusions

The possibility of commercial aluminum bronzes to present the thermoelastic martensitic transformation and its origin in shape memory phenomena was investigated in this work. It was observed that a small compositional modification in these commercial materials can promote the occurrence of thermoelastic transformation, which was confirmed through a DSC thermal analysis. Modified bronze alloys, now classified as Cu-Al-Ni SMA, present M_s temperatures in the range of 40°C to 190°C, depending on the Al content. The hardness HV results showed that the modified samples, before and after quenching, exhibit a lower hardness value than the as supplied bronzes (after quenching) due to the occurrence of the twinned martensite phases. The XRD results confirmed the presence of the twinned martensite phases, which is the phase that promotes the shape memory phenomena. Images from the optical microscopy allowed the observation of the studied alloys microstructure, confirming the presence of the martensite phases for the modified and quenched alloys (Cu-Al-Ni SMA). In conclusion, this work has shown that commercial bronze alloys can be modified to be used as SMA, and the BMT alloy presented the best results concerning the transformation temperatures (between 30°C and 180°C) and thermal stability of the martensitic thermoelastic transformation.

5. Acknowledgements

The authors thank the National Council for Scientific and Technological Development (CNPq) Brazilian office for sponsoring the following projects: National Institute of Science and Technology for Smart Structures in Engineering (INCT-EIE, grant number 574001/2008-5), UFCG-UFRJ-ITA "Casadinho-Procad" (grant number 552199/2011-7), Universal 14/2012 (grant number 474524/2012-4) and PQ-1D (grant number 304658/2014-6).

6. References

1. Otsuka K, Wayman CM. *Shape Memory Materials*. 1st ed. Cambridge: Cambridge University Press; 1998. 284 p.
2. Patoor E, Lagoudas DC, Entchev PB, Brinson LC, Gao X. Shape memory alloys, Part I: General properties and modeling of single crystals. *Mechanics of Materials*. 2006;38(5-6):391-429.
3. Pereira EC, Matlakhova LA, Matlakhov AN, Araújo CJ, Shigue CY, Monteiro SN. Reversible martensite transformations in thermal cycled polycrystalline Cu-13.7%Al-4.0%Ni alloy. *Journal of Alloys and Compounds*. 2016;688(Pt B):436-446.
4. Yang S, Zhang F, Wu J, Lu Y, Shi Z, Wang C, et al. Superelasticity and shape memory effect in Cu-Al-Mn-V shape memory alloys. *Materials & Design*. 2017;115:17-25.
5. Chang SH. Influence of chemical composition on the damping characteristics of Cu-Al-Ni shape memory alloys. *Materials Chemistry and Physics*. 2011;125(3):358-363.
6. Pereira EC, Matlakhova LA, Matlakhov AN, Shigue CY, Monteiro SN. Physical and Structural Characterization of a Monocrystalline Cu-13.7Al-4.2Ni Alloy Subjected to Thermal Cycling Treatments. *Metallurgical and Materials Transactions A*. 2014;45(4):1866-1875.
7. Copper Development Association. *Aluminium Bronze - Essential for Industry*. CDA Publication Nº 86. Hemel Hempstead: Copper Development Association; 1989. 16 p.
8. Araujo VEA, Gastien R, Zelaya E, Beiroa JI, Corro I, Sade M, et al. Effects on the martensitic transformations and the microstructure of CuAlNi single crystals after ageing at 473 K. *Journal of Alloys and Compounds*. 2015;64:155-161.
9. Lelatko J, Morawiec N, Koval YN, Kolomyttsev VI. Structure and properties of high-temperature alloys with the effect of shape memory in the system Cu-Al-Nb. *Metal Science and Heat Treatment*. 2009;41(8):351-353.
10. Lin G, Wang H, Wei Y, Zhang Z, Zhou K. Effects of heat treatments on microstructure and properties of nickel-aluminum bronze fabricated by centrifugal casting. *Journal of Materials Research*. 2016;31(24):3832-3840.
11. Silva NJ, Silva MM, Gomes AAC, Santos MA, Gonzalez CH, De Araujo CJ. Influência do reprocessamento por plasma e da variação do tempo de tratamento térmico nas propriedades de uma liga Cu-Al-Ni com memória de forma. 17º CBECIMat - Congresso Brasileiro de Engenharia e Ciência dos Materiais. 2006 Nov 15-19; Foz do Iguaçu, PR, Brazil. p. 5264-5275
12. Chentouf SM, Bouabdallah M, Gachon JC, Patoor E, Sari A. Microstructural and thermodynamic study of hypoeutectoidal Cu-Al-Ni shape memory alloys. *Journal of Alloys and Compounds*. 2009;470(1):507-514.
13. Rodrigues CA, Melo MLNM, Paes LES. Caracterização de uma liga de bronze de alumínio submetida a diferentes tratamentos térmicos. *Rem: Revista Escola de Minas*. 2012;65(3):343-348.